



12



TECHNICAL REPORT N-76-9

A METHOD FOR DESIGNING DEEP UNDERGROUND STRUCTURES SUBJECTED TO DYNAMIC LOADS

by

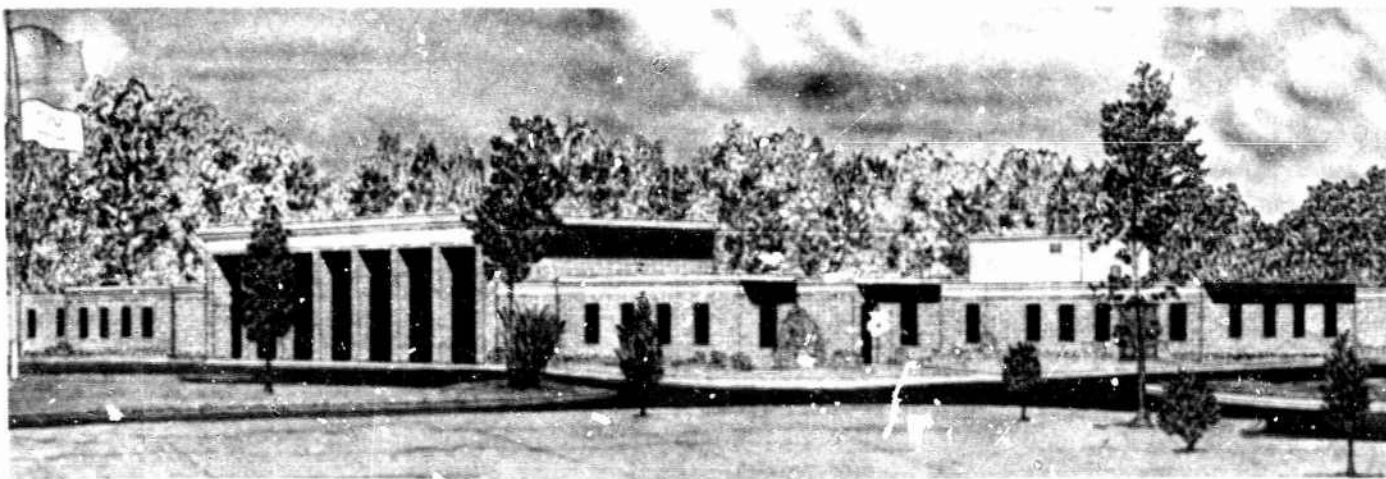
James L. Drake, James R. Britt

Weapons Effects Laboratory
U. S. Army Engineer Waterways Experiment Station
P. O. Box 631, Vicksburg, Miss. 39180

September 1976

Final Report

Approved For Public Release; Distribution Unlimited



Prepared for Defense Nuclear Agency, Washington, D. C. 20305 and
Office, Chief of Engineers, U. S. Army
Washington, D. C. 20314

Under DNA Subtask J34CAXSX311, "Underground Structures
Studies," and OCE Project 4A762719AT40-A1-017,
"Stability of Deep Underground Structures in Rock"

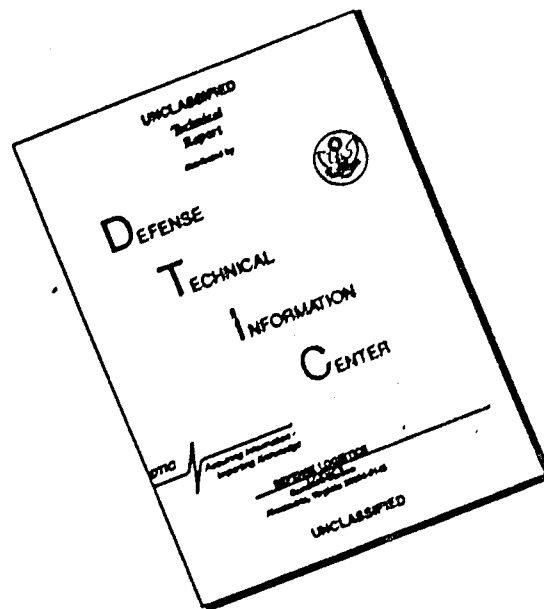
D D C

OCT 12 1976

A

Destroy this report when no longer needed. Do not return
it to the originator.

DISCLAIMER NOTICE



THIS DOCUMENT IS BEST QUALITY AVAILABLE. THE COPY FURNISHED TO DTIC CONTAINED A SIGNIFICANT NUMBER OF PAGES WHICH DO NOT REPRODUCE LEGIBLY.

Unclassified

SECURITY CLASSIFICATION OF THIS PAGE (When Data Entered)

REPORT DOCUMENTATION PAGE		READ INSTRUCTIONS BEFORE COMPLETING FORM
1. REPORT NUMBER Technical Report N-76-9 ✓	2. GOVT ACCESSION NO.	3. RECIPIENT'S CATALOG NUMBER 14 WES-TR-N-76-9
4. TITLE (and Subtitle) A METHOD FOR DESIGNING DEEP UNDERGROUND STRUCTURES SUBJECTED TO DYNAMIC LOADS		5. TYPE OF REPORT & PERIOD COVERED Final report
7. AUTHOR(s) James L. Drake James R. Britt		6. PERFORMING ORG. REPORT NUMBER
9. PERFORMING ORGANIZATION NAME AND ADDRESS U. S. Army Engineer Waterways Experiment Station Weapons Effects Laboratory P. O. Box 631, Vicksburg, Miss. 39180		8. CONTRACT OR GRANT NUMBER(s)
11. CONTROLLING OFFICE NAME AND ADDRESS Defense Nuclear Agency, Washington, D. C. 20305 and Office, Chief of Engineers, U. S. Army Washington, D. C. 20314		10. PROGRAM ELEMENT, PROJECT, TASK AREA & WORK UNIT NUMBERS DNA Subtask J34CAXSX311 and OCE Project 4A762719AT40/A1/017
14. MONITORING AGENCY NAME & ADDRESS (if different from Controlling Office)		12. REPORT DATE September 1976
		13. NUMBER OF PAGES 28
		15. SECURITY CLASS. (of this report) Unclassified
		15a. DECLASSIFICATION/DOWNGRADING SCHEDULE
16. DISTRIBUTION STATEMENT (of this Report) Approved for public release; distribution unlimited. DA-4-A-762711-AT-40		
17. DISTRIBUTION STATEMENT (of the abstract entered in Block 20, if different from Report)		
18. SUPPLEMENTARY NOTES		
19. KEY WORDS (Continue on reverse side if necessary and identify by block number) Dynamic loads Underground structures		
20. ABSTRACT (Continue on reverse side if necessary and identify by block number) This report describes solutions to a class of dynamic elastoplastic problems that model some of the salient features of the response of hardened underground facilities in rock. The theoretical model consisted of multilayered concentric cylinders of elastoplastic materials with time-dependent loads applied to the exterior boundary. Each element in the cross section was assumed to be incompressible and its yield governed by a Mohr-Coulomb failure criterion. The number of elements within the cross section was not limited. Solutions (Continued)		

DD FORM 1 JAN 73 1473

EDITION OF 1 NOV 65 IS OBSOLETE

Unclassified

SECURITY CLASSIFICATION OF THIS PAGE (When Data Entered)

100

Unclassified

SECURITY CLASSIFICATION OF THIS PAGE(When Data Entered)

20. ABSTRACT (Continued).

of the theoretical model were cast in the general form normally used in structural dynamics:

$$\text{Mass} \times \text{Acceleration} = \text{External applied load} - \text{Internal resistance} .$$

The resulting equations can be quickly and inexpensively evaluated on a digital computer.

To extend the range of validity of the exact theory, a first-order correction factor was developed to account for the compressibility of the materials, and a simple method to treat backpacked structures was introduced.

The theory was verified by comparing calculated values with experimental measurements from small-scale static and explosively driven tunnel collapse studies. Good agreement was noted for all cases considered.

Unclassified

SECURITY CLASSIFICATION OF THIS PAGE(When Data Entered)

PREFACE

This report presents results of a theoretical study which evaluates the response of hardened underground facilities in rock to dynamically applied loads produced by explosions. This research was conducted by personnel of the Phenomenology and Effects Division (PED) of the Weapons Effects Laboratory (WEL), U. S. Army Engineer Waterway Experiment Station (WES), during the period January 1975-January 1976.

The primary analytical development and preparation of the initial draft report were sponsored by the Defense Nuclear Agency under Subtask J34CAXSX311, "Underground Structures Studies," under the guidance of Dr. Kent Goering. Final report preparation and additional analytical work including investigations of backpacking and unloading and subsequent reloading were sponsored by the Office, Chief of Engineers, under Project 4A762719AT40/A1/017, "Stability of Deep Underground Structures in Rock," which was monitored by Mr. D. S. Reynolds.

This report was written by Messrs. J. L. Drake and J. R. Britt, PED, under the general supervision of Mr. L. F. Ingram, Chief, PED, and Mr. W. J. Flathau, Chief, WEL.

COL G. H. Hilt, CE, and COL J. L. Cannon, CE, were Directors of WES during the preparation and publication of this report. Mr. F. R. Brown was Technical Director.

CONTENTS

PREFACE-----	1
CONVERSION FACTORS, U. S. CUSTOMARY TO METRIC (SI)	
UNITS OF MEASUREMENT-----	3
CHAPTER 1 INTRODUCTION-----	4
1.1 Background-----	4
1.2 Objective-----	5
1.3 Approach-----	5
CHAPTER 2 THEORY-----	7
2.1 Problem Formulation-----	7
2.1.1 Field Equations-----	7
2.1.2 Material Models-----	9
2.1.3 Boundary Conditions-----	11
2.2 Problem Solutions-----	11
2.2.1 Elastic Region-----	11
2.2.2 Plastic Region-----	12
2.2.3 Generalized Stress Distribution-----	13
2.2.4 Stress Solution-----	14
2.2.5 Elastic-Plastic Boundaries-----	16
2.3 A First-Order Compressibility Correction-----	18
2.4 A Summary of the Computational Method-----	19
2.5 Treatment of Backpacked Structures-----	19
2.6 Discussion of Unloading-----	20
CHAPTER 3 EVALUATION OF THE THEORY-----	21
3.1 Comparison of Calculations with Experimental Evidence-----	21
3.2 Conclusions-----	24
REFERENCES-----	27
APPENDIX A: NOTATION-----	28
TABLE	
3.1 Material Properties Used in the Calculations-----	26
FIGURES	
2.1 Geometry of rock-liner system-----	8
3.1 Calculated displacement-time curves compared with measurements with 80-gram charges-----	22
3.2 Theoretical and experimental wall displacements versus time for three pressure pulses-----	23
3.3 Computed and measured static tunnel closure versus pressure-----	24

CONVERSION FACTORS, U. S. CUSTOMARY TO METRIC (SI)
UNITS OF MEASUREMENT

U. S. customary units of measurement used in this report can be converted to metric (SI) units as follows:

<u>Multiply</u>	<u>By</u>	<u>To Obtain</u>
mils	0.00254	centimetres
inches	2.54	centimetres
pounds (force) per square inch	6.894757	kilopascals
kilobars	100.00	megapascals
inches per second per second	2.54	centimetres per second per second
degrees (angle)	0.01745329	radians

A METHOD FOR DESIGNING DEEP UNDERGROUND
STRUCTURES SUBJECTED TO DYNAMIC LOADS

CHAPTER 1

INTRODUCTION

1.1 BACKGROUND

Design of superhard underground facilities to resist the shock levels induced by nuclear weapons must take full advantage of the strength of the surrounding rock. Survival at levels in excess of 2 kbars¹ has been demonstrated by experiments in an idealized hard rock medium. In principle, additional hardness can be achieved by placing the facility deep enough to attenuate the shock to levels that can be resisted by structural hardening procedures.

Static methods are now being used for design of hardened underground facilities. Perhaps the best analytical procedure is that outlined by N. M. Newmark (Reference 1) wherein rock and liner systems are treated as elastoplastic materials that obey a general form of the Mohr-Coulomb failure criterion. Incompressible plastic strains and axially symmetric stresses are assumed. This analysis proceeds from the interior of the lining-medium system where the circumferential strain and radial stress are known, and successively works the solution outward by matching stresses and displacements across liner junctions and finally the rock-liner interface to obtain the free-field conditions in the rock. Similarly, it is possible to work from known conditions on any interior element inward or outward, but not from the free-field stress situation.

A. J. Hendron, Jr., and A. K. Aiyer (Reference 2) have extended Newmark's static analysis to include dilatancy of the Mohr-Coulomb material at failure. These authors report, however, that the increase in volume predicted by their theory is too large compared with experimental

¹ A table of factors for converting U. S. customary units of measurement to metric (SI) units is presented on page 3.

evidence in real rocks. They claim that values of radial displacement calculated by their theory are a conservative upper bound. On the other hand, Newmark's analysis, which neglects any volume change due to the plastic strains at failure, predicts radial displacements that are too small and should be used as a lower bound.

Sophisticated computer codes are available that can account for the complex interactions of the structural elements under dynamic loading. General stress-strain relationships that closely model the real material behavior in both the elastic and inelastic regions can be used in these types of codes. However, these procedures are still too complex and time-consuming to be useful for design but should be useful for final analysis after a preliminary design has been proposed.

Treating the dynamic load as an equivalent static load is acceptable for use in structural design methods. In the case of normal structural elements (columns, beams, etc.), the equivalent static loading may be determined from a dynamic response chart for various ratios of the duration of loading to the natural period of the structure. For rock tunnel and liner systems the natural period is not easily defined without a dynamic analysis of the entire system.

1.2 OBJECTIVE

The goal of this report is to develop solutions for a class of dynamic problems that have direct bearing on design considerations for deep underground facilities in rock. Specifically, an extension of the static methods outlined by Newmark to accommodate dynamic loads is sought.

1.3 APPROACH

This report describes solutions to a class of dynamic elastoplastic problems that model some of the salient features of the response of hardened underground facilities in rock. The theoretical model consists of multilayered concentric cylinders of elastoplastic materials with time-dependent loads applied to the exterior boundary. Each element in the cross section is assumed to be incompressible and its yield governed by a Mohr-Coulomb failure criterion. The number of elements within the

cross section is not limited. Solutions of the theoretical model are cast in the general form normally used in structural dynamics:

$$\text{Mass} \times \text{Acceleration} = \text{External applied load} - \text{Internal resistance}$$

The resulting equations can be quickly and inexpensively evaluated on a digital computer.

To extend the range of validity of this exact theory, a first-order correction factor was developed to account for the compressibility of the materials, and a simple method to treat backpacked structures was introduced. The theory was then verified by comparing calculated values with experimental measurements from small-scale static and explosively driven tunnel collapse studies.

CHAPTER 2

THEORY

2.1 PROBLEM FORMULATION

The rock and liner system is modeled as multilayered concentric cylinders of elastoplastic materials in plane strain (see Figure 2.1). An arbitrary time-dependent pressure is applied to the outer boundary, and an arbitrary pressure, also time-dependent if desired, is applied to the internal boundary. It is assumed that the materials in the cross section are incompressible in both the elastic and the plastic states. (As discussed in Section 2.3, a first-order compressibility correction is easily incorporated.) With these assumptions, the effects of material compaction and stress wave interaction within the cross section are neglected, thereby greatly simplifying the analysis. The number of material layers in this analysis is unlimited.

2.1.1 Field Equations. Equations requiring equilibrium and conservation of mass are basic to any analytical study of structural response. Solutions to these equations are valid in both the elastic and plastic states of the material.

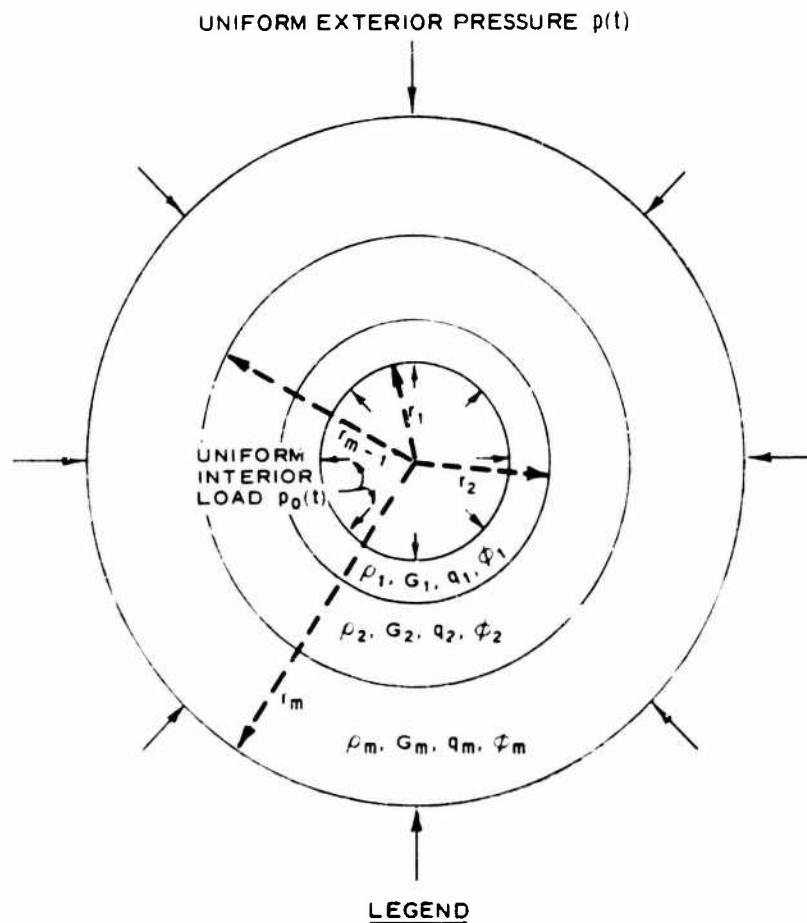
The equation of motion in polar coordinates is as follows:¹

$$\frac{\partial \sigma_r^i}{\partial r} + \frac{\sigma_r^i - \sigma_\theta^i}{r} = \rho_i \left(\frac{\partial^2 u_r^i}{\partial t^2} \right) \quad (i = 1, 2, \dots, m) \quad (2.1)$$

where

- σ_r^i = radial stress component
- r = radial coordinate
- σ_θ^i = tangential stress component
- ρ_i = mass density
- u_r^i = radial displacement component
- t = time

¹ For convenience, symbols and unusual abbreviations are listed and defined in the Notation (Appendix A).



- LEGEND**
- r_1, r_2 = INTERIOR BOUNDARIES OF THE FIRST AND SECOND MATERIAL LAYERS, RESPECTIVELY
 - m = NUMBER OF MATERIALS IN THE CROSS SECTION
 - ρ = DENSITY
 - G = SHEAR MODULUS
 - q = COHESION
 - ϕ = ANGLE OF INTERNAL FRICTION

Figure 2.1 Geometry of rock-liner system.

i = subscript or superscript referring to a component material in the cross section

m = number of materials in the cross section

This equation can be solved when relationships between stresses and displacements (constitutive laws) are given. In the plastic state an additional equation given by the yield criterion relating the radial and tangential stresses is necessary for a complete solution.

Incompressibility requires the conservation of mass to be

$$\frac{\partial u_r^i}{\partial r} + \frac{u_r^i}{r} = 0 \quad (i = 1, 2, \dots, m) \quad (2.2)$$

The general solution to Equation 2.2 is

$$u_r^i = \frac{U^i(t)}{r} \quad (2.3)$$

where $U^i(t)$ is a general function of time to be determined from the boundary conditions. It is evident from Equation 2.3 that if the displacement field is continuous between component materials, $U^i(t)$ must be the same for all materials. Thus, the superscript i is dropped such that

$$U^1(t) = U^2(t) = \dots = U(t) \quad (2.4)$$

2.1.2 Material Models. Stress-strain relationships for an incompressible elastic medium in plane strain can be written as

$$\begin{aligned} \sigma_r^i &= S^i + 2G_i \epsilon_r^i \\ \sigma_\theta^i &= S^i + 2G_i \epsilon_\theta^i \\ \sigma_z^i &= S^i \end{aligned} \quad (2.5)$$

where

S^i = mean normal stress

G_i = shear modulus

ϵ_r^i = radial strain component
 ϵ_θ^i = tangential strain component
 σ_z^i = axial stress component

and the mean normal stress is given by

$$s^i = \frac{1}{3} \left(\sigma_r^i + \sigma_\theta^i + \sigma_z^i \right)$$

In polar coordinates, the strains are defined as

$$\begin{aligned}
 \epsilon_r^i &= \frac{\partial u_r^i}{\partial r} = - \frac{U(t)}{r^2} \\
 \epsilon_\theta^i &= \frac{u_r^i}{r} = \frac{U(t)}{r^2}
 \end{aligned} \tag{2.6}$$

where the radial displacement given by Equation 2.3 is substituted into the strain definitions. Because $U(t)$ is independent of the state of the material, it is evident that Equations 2.6 are valid in both the elastic and plastic regions.

Stress-strain relations in the plastic region are implied and defined by the condition of incompressibility and from the form of the yield law. A Mohr-Coulomb yield criterion assumed for all the component materials is given as

$$\left(\sigma_r^i - \sigma_\theta^i \right) = \sigma_r^i (1 - N_i) + 2q_i \sqrt{N_i} \tag{2.7}$$

where

$$N_i = \tan^2 \left(45^\circ + \frac{\phi_i}{2} \right) = \frac{1 + \sin \phi_i}{1 - \sin \phi_i}$$

and q_i is the cohesion and ϕ_i is the angle of internal friction. The assumption of incompressibility is not strictly compatible with this yield criterion except for $\phi_i = 0$ (von Mises yield criteria) unless a nonassociative flow rule is assumed. Mohr-Coulomb materials dilate while undergoing failure; however, neglecting this effect is not

expected to affect the results greatly, and simplifies the solution.

2.1.3. Boundary Conditions. Stresses and displacements are assumed to be continuous across the various internal boundaries between materials. Further, dynamic pressures are applied at the exterior and interior boundaries. The external pressure was assumed to be much greater than the interior pressure, causing the deformation to be inward. These boundary conditions can be expressed as

$$\left. \begin{aligned} \sigma_r^1 &= -p_o(t) \quad \text{at } r = r_1 \\ \sigma_r^i &= \sigma_r^{i+1} \\ u_r^i &= u_r^{i+1} \end{aligned} \right\} \quad \text{at } r = r_{i+1} \quad (i = 1, 2, \dots, m-1)$$

$$\sigma_r^m = -p(t) \quad \text{at } r = r_{m+1} \quad (2.8)$$

where

$p_o(t)$ = internal pressure (compressive)

r_i = interior boundary of the i^{th} material layer

$p(t)$ = external pressure-time history (compressive)

all of which are depicted in Figure 2.1.

Additional internal boundary conditions may occur if any of the component materials are partially elastic and partially plastic. Across this elastic-plastic boundary

$$(\sigma_r - \sigma_\theta)_{\text{elastic}}^i = (\sigma_r - \sigma_\theta)_{\text{plastic}}^i$$

and the normal stresses σ_r^i are continuous.

2.2 PROBLEM SOLUTIONS

Solutions to the equation of motion (Equation 2.1) are possible from the displacement solution (Equation 2.3) and either the stress-strain relations in the elastic region (Equation 2.5) or the yield criterion (Equation 2.7) in the plastic region.

2.2.1 Elastic Region. In the elastic region, the following

equation is obtained from the elastic stress-strain relations and from Equations 2.6:

$$\sigma_r^i - \sigma_\theta^i = -4G_i \left[\frac{U(t)}{r^2} \right]$$

Substituting this expression into the equation of motion (Equation 2.1) gives

$$\frac{\partial \sigma_r^i}{\partial r} - 4G_i \left[\frac{U(t)}{r^3} \right] = \frac{\rho_i}{r} \left[\frac{d^2 U(t)}{dt^2} \right]$$

with the solution

$$\sigma_r^i = \rho_i \ln \left(\frac{r}{r_i} \right) \left[\frac{d^2 U(t)}{dt^2} \right] - \frac{2G_i}{r_i^2} \left(\frac{r_i}{r} \right)^2 U(t) + C_i \quad (2.9)$$

where C_i is a constant independent of r to be determined from boundary conditions. From this result and Equations 2.5 and 2.6 the mean normal stress S^i is given by

$$S^i = \sigma_r^i + \left(\frac{2G_i}{r_i^2} \right) \left(\frac{r_i}{r} \right)^2 U(t) \quad (2.10)$$

2.2.2 Plastic Region. An expression for the stress difference $(\sigma_r^i - \sigma_\theta^i)$ in the plastic region is given by the yield condition (Equation 2.7). Substituting this relationship into the equation of motion (Equation 2.1) yields

$$\frac{\partial \sigma_r^i}{\partial r} + \frac{\sigma_r^i}{r} (1 - N_i) = \frac{1}{r} \left\{ \rho_i \left[\frac{d^2 U(t)}{dt^2} \right] - 2q_i \sqrt{N_i} \right\}$$

with the solution

$$\sigma_r^i = \left\{ \rho_i \left[\frac{d^2 U(t)}{dt^2} \right] - 2q_i \sqrt{N_i} \right\} \left(\frac{1}{1 - N_i} \right) \left[1 - \left(\frac{r}{r_i} \right)^{N_i - 1} \right] + C_i \left(\frac{r}{r_i} \right)^{N_i - 1} \quad (2.11)$$

Note that

$$\lim_{n_i \rightarrow 0} \frac{1}{n_i} \left[\left(\frac{r}{r_i} \right)^{n_i} - 1 \right] = \ln \left(\frac{r}{r_i} \right)$$

$$\lim_{n_i \rightarrow 0} \left(\frac{r}{r_i} \right)^{n_i} = 1$$

where $n_i = N_i - 1$. Thus, in the limit as $N_i \rightarrow 1$ or $\phi_i \rightarrow 0$, the expressions for the elastic stress distribution (Equation 2.9) and plastic distributions (Equation 2.11) bear similar terms for the inertial contribution and for the arbitrary constant C_i .

2.2.3 Generalized Stress Distribution. Since each material is allowed to be elastic or plastic or even partially yielded, the number of stress combinations required to solve the boundary conditions for the constant C_i is m^2 for m materials in the cross section. This situation can be avoided by writing a more general stress distribution which can be used in both the elastic and plastic regions. This generalized stress distribution is expressed in operator form as

$$\sigma_r^i = \left\{ \frac{\rho_i}{n_i} \left[\left(\frac{r}{r_i} \right)^{n_i} - 1 \right] \frac{d^2}{dt^2} - \frac{2G_i}{r_i^2} \left(\frac{r_i}{r} \right)^2 \right\} U(t) - \left(\frac{2q_i}{n_i} \right) \sqrt{(n_i + 1)} \left[\left(\frac{r}{r_i} \right)^{n_i} - 1 \right] + C_i \left(\frac{r}{r_i} \right)^{n_i} \quad (2.12)$$

where

$$n_i = N_i - 1 = \frac{2 \sin \phi_i}{1 - \sin \phi_i}$$

and again noting

$$\lim_{n_i \rightarrow 0} \frac{1}{n_i} \left[\left(\frac{r}{r_i} \right)^{n_i} - 1 \right] = \ln \left(\frac{r}{r_i} \right)$$

In the elastic state it is necessary to define $n_i = q_i = 0$ for Equation 2.12 to be valid. The plastic state requires $G_i = 0$ to obtain the

correct stresses. Using Equation 2.12 in the boundary conditions will yield a generalized form for the constant C_i which is valid in either the elastic or plastic state and which correctly accounts for the states of all m elements.

2.2.4 Stress Solution. Substituting Equation 2.12 into the boundary conditions expressed by Equations 2.8 gives the following recurrence formulas for C_i :

$$C_1 = -p_o(t) + \frac{2G_1}{r_1^2} U$$

$$C_{i+1} = \frac{\rho_i}{n_i} \left[\left(\frac{r_{i+1}}{r_i} \right)^{n_i} - 1 \right] \frac{d^2 U}{dt^2} - \frac{2G_i}{r_i^2} \left(\frac{r_i}{r_{i+1}} \right)^2 U + \frac{2G_{i+1} U}{r_{i+1}^2}$$

$$- \frac{2q_i}{n_i} \sqrt{n_i + 1} \left[\left(\frac{r_{i+1}}{r_i} \right)^{n_i} - 1 \right] + C_i \left(\frac{r_{i+1}}{r_i} \right)^{n_i} \quad (2.13)$$

Completing this solution and continuing the recurrence out to $r = r_{m+1}$ gives the following formula:

$$\sigma_r^i = \left\{ \frac{\rho_i}{n_i} \left[\left(\frac{r}{r_i} \right)^{n_i} - 1 \right] + \left(\frac{r}{r_i} \right)^{n_i} M_{i-1} \right\} \frac{d^2 U}{dt^2}$$

$$+ \left\{ \frac{2G_i}{r_i^2} \left[\left(\frac{r}{r_i} \right)^{n_i+2} - 1 \right] + \left(\frac{r}{r_i} \right)^{n_i} K_{i-1} \right\} U$$

$$- \left\{ \left(\frac{2q_i}{n_i} \right) \sqrt{n_i + 1} \left[\left(\frac{r}{r_i} \right)^{n_i} - 1 \right] + \left(\frac{r}{r_i} \right)^{n_i} (Y_{i-1} + P_{oi-1}) \right\} \quad (2.14)$$

where

$$\begin{aligned}
 M_i &= \sum_{j=1}^i \frac{\rho_j}{n_j} \left[\left(\frac{r_{j+1}}{r_j} \right)^{n_i} - 1 \right] \prod_{k=j+1}^i \left(\frac{r_{k+1}}{r_k} \right)^{n_k} \\
 Y_i &= \sum_{j=1}^i \left\{ \left(\frac{2q_i}{n_j} \right) \sqrt{n_j + 1} \left[\left(\frac{r_{j+1}}{r_j} \right)^{n_j} - 1 \right] \right\} \prod_{k=j+1}^i \left(\frac{r_{k+1}}{r_k} \right)^{n_k} \\
 K_i &= \sum_{j=1}^i \frac{2G_j}{r_{j+1}^2} \left[\left(\frac{r_{j+1}}{r_j} \right)^{n_j+2} - 1 \right] \prod_{k=j+1}^i \left(\frac{r_{k+1}}{r_k} \right)^{n_k} \\
 P_{oi} &= p_o(t) \prod_{k=1}^i \left(\frac{r_{k+1}}{r_k} \right)^{n_k}
 \end{aligned} \tag{2.15}$$

and

$$M \left(\frac{d^2 U}{dt^2} \right) = \left[P_o(t) - p_o(t) \right] - (KU - Y) \tag{2.16}$$

where

- $M = M_m$ = effective mass
- $P_o = P_{om}$ = effective interior pressure
- $K = K_m$ = effective elastic stiffness
- $Y = Y_m$ = effective rigid plastic collapse pressure of the m materials

The symbol $\sum_{j=1}^i$ denotes a sum of terms with $j = 1$ to $j = i$, and

$\prod_{k=j+1}^i$ denotes a product of terms with $k = j + 1$ to $k = i$.

Equations 2.14-2.16 along with the yield condition (Equation 2.7) completely describe the stresses and motions of the rock-liner system

under dynamic loading. The differential Equation 2.16 is of the same form as that used in structural dynamics:

$$\begin{aligned} \text{Mass} \times \text{Acceleration} &= \text{External applied} \\ &\text{load} - \text{Internal resistance} \end{aligned}$$

In this case, the internal load-resistance function is $R = KU - Y$. Note that initially $Y = 0$ and the resistance is due to the elastic stiffness K . As the external applied load increases, elements begin to fail, effectively increasing Y as K decreases until the applied load is such that the entire section fails, the full value of Y is reached, and $K = 0$.

2.2.5 Elastic-Plastic Boundaries. Solutions expressed by Equations 2.14 and 2.16 are valid for all load conditions in both the elastic and plastic ranges as long as the deformations are inward; however, these equations alone are not sufficient to describe the stresses and motions of the rock-liner system. Yield conditions must be used along with these equations to determine the elastic-plastic state of the system.

When the deformation is inward, yielding in each of the component materials begins at the interior boundary and progresses outward until the entire element is fully plastic. This behavior can be used to simplify the analysis as follows. Divide each component material into two parts, the inner portion with only plastic properties and the outer shell with elastic properties. With this definition the m materials are divided into two m layers where

$$\left. \begin{array}{l} n_i \\ q_i \end{array} \right\} = 0 \quad \text{for even values of } i$$

$$G_i = 0 \quad \text{for odd values of } i \quad (2.17)$$

and r_{i+1} for odd values of i is the elastic-plastic interface. A material is fully elastic when $r_{i+1} = r_i$ for odd values of i and

a material is fully plastic when $r_{i+1} = r_{i+2}$ for odd values of i . Using these definitions, the elastic-plastic boundary, r_{i+1} for odd values of i , can be calculated from the yield conditions.

Continuity of stresses across the elastic-plastic interface requires that

$$\left(\sigma_r^{i+1} - \sigma_\theta^{i+1} \right) = \left(\sigma_r^i - \sigma_\theta^i \right) \quad \text{at } r = r_{i+1} \quad \text{for odd values of } i$$

Using Equations 2.5 and 2.6 in the elastic range and Equation 2.7 in the plastic region gives

$$-\frac{4G_{i+1}}{r_i^2} \left(\frac{r_i}{r_{i+1}} \right)^2 U = -n_i \sigma_r^i + 2q_i \sqrt{n_i + 1} \quad \text{at } r = r_{i+1}$$

for odd values of i

Substituting in this result the solution for radial stresses (Equation 2.14) yields the expression for r_{i+1}/r_i and $i = \text{odd}$

$$\begin{aligned} -\frac{4G_{i+1}}{r_i^2} \left(\frac{r_i}{r_{i+1}} \right)^2 U = & -\left(\frac{r_{i+1}}{r_i} \right)^{n_i} \left[(\rho_i + n_i M_{i-1}) \left(\frac{d^2 U}{dt^2} \right) \right. \\ & \left. + n_i (K_{i-1} U - Y_{i-1} - P_{oi-1}) - 2q_i \sqrt{n_i + 1} \right] + \rho_i \left(\frac{d^2 U}{dt^2} \right) \end{aligned} \quad (2.18)$$

For $n_i = 0$ this equation reduces to the simple form

$$\left(\frac{r_{i+1}}{r_i} \right)^2 = \frac{-2G_{i+1} U}{q_i r_i^2} \quad (2.19)$$

Note that for the Mohr-Coulomb failure criterion, inertial mass \times acceleration terms appear in the condition for dynamic failure. Until the time at which the maximum inward particle velocity is reached, when $d^2 U/dt^2 \leq 0$, the inertial forces tend to strengthen the section causing r_{i+1}/r_i to be less than its static value. However, when $d^2 U/dt^2 > 0$,

these forces cause the plastic boundary to grow outward more rapidly than under static load.

2.3 A FIRST-ORDER COMPRESSIBILITY CORRECTION

For static loading and elastic response the ratio of the compressible to the incompressible radial displacements is (Reference 3)

$$\frac{u_c}{u_i} = 1 + (1 - 2\nu)r^2 \left[\frac{r_2^2 p_2 - r_1^2 p_1}{r_1^2 r_2^2 (p_2 - p_1)} \right]$$

where ν is Poisson's ratio of the material, r_1 and p_1 are the inside radius and applied load, respectively, and r_2 and p_2 are the outside radius and applied load, respectively. For most tunnel liners being considered, $p_1 = 0$ (atmospheric pressure) so that p_1/p_2 is very small. Expanding the expression for u_c/u_i evaluated at $r = r_1$ in powers of p_1/p_2 gives

$$\frac{u_c(r_1)}{u_i(r_1)} = 1 + (1 - 2\nu) \left\{ 1 + \left[1 - \left(\frac{r_1}{r_2} \right)^2 \right] \sum_{n=1}^{\infty} \left(\frac{p_1}{p_2} \right)^n \right\}$$

For $p_1/p_2 \approx 0$ this expression becomes

$$\frac{u_c(r_1)}{u_i(r_1)} = 2(1 - \nu) \quad (2.20)$$

When p_1 is zero, this ratio is exact for the static elastic case. Experience indicates that this is also a reasonably accurate, first-order correction factor for the dynamic displacements of an elastic-plastic rock-tunnel liner system. In this application an average value of the Poisson's ratios of the component materials should be used. Typically, ν for common rock and liner materials ranges from about 0.2 to 0.3, and $u_c(r_1)/u_i(r_1)$ ranges from 1.6 to 1.4. Average values of $\nu = 0.25$ and $u_c(r_1)/u_i(r_1) = 1.5$ are adequate for most calculations.

2.4 A SUMMARY OF THE CALCULATIONAL METHOD

Equations 2.18 or 2.19 together with the equation of motion, 2.16, can be solved for $U(t)$ by a numerical integration such as the Runge-Kutta method. Then using Equation 2.6 and the compressibility correction, Equation 2.20, the radial displacement can be determined. The radial stress component is given by Equations 2.14 and 2.15; then with the mean normal stress S^i given in Equation 2.10, the other stress components are given in Equations 2.5 and 2.7. Thus, these relations provide a complete description of the stresses and motions of the rock-liner system in a form suitable for fast computer calculations.

2.5 TREATMENT OF BACKPACKED STRUCTURES

Backpacking is commonly a crushable material, such as foamed concrete, placed between the rock and the tunnel liner to absorb the large strains suffered by the rock and, consequently, to isolate the liner from excessive damage. The simplest treatment of backpacking is the hydrostatic model, which neglects the shear strength of the material. Thus the pressures at the inside and outside of the backpacking are the same. Experimental pressure-volumetric strain curves can be used in this model to calculate the pressure on the rock and liner. A simple iterative process can be set up which links the radial displacement of the liner to the displacement of the rock as a function of volume changes in the backpacking. Since the present analysis allows a time-varying interior pressure $p_o(t)$, the calculational method is easily adapted for computations using this hydrostatic model of backpacking. The computer code presently in use at the U. S. Army Engineer Waterways Experiment Station includes this option.

For free-field stresses in the rock which are essentially axisymmetric (uniform radial load), the hydrostatic model provides an accurate description of the backpacking collapse. The effect of shear strength of the backpacking on rock-liner displacements is negligibly small in this case.

For the biaxial free-field stresses in which the difference between the vertical and horizontal normal stress components is large compared

with the collapse strength of the backpacking, the hydrostatic model of collapse of the backpacking is no longer valid for relatively large rock deformations. Since the material cannot flow to equalize the stresses, ovaling of the backpacking results, transmitting highly nonuniform radial loads to the liner which may collapse prematurely.

2.6 DISCUSSION OF UNLOADING

The present analysis is limited to monotonically increasing displacements. In the case of small plastic strains, unload and a subsequent reload may take place elastically which can be treated simply within the present analysis. For von Mises materials in static loading, Prager and Hodge (Reference 3) give equations for both elastic and plastic unload. The plastic unload of a Mohr-Coulomb material may be treated in a similar manner; but the analysis is more complex than the von Mises case, as the authors of the present report have found in a thorough study of this process. In the present study it was discovered that the Mohr-Coulomb plastic unloading often involves further yielding of the material even as the inward displacement decreases. The manner and extent of this unload yielding depend primarily on (1) the amount of plastic deformation in the material at the end of the load phase and (2) the confining pressure at the interior of the layer of material. The resulting equations are mathematically too cumbersome to be included in the analysis of this report. The experience gained in this study indicates that elastic unload is often a good first approximation for the purposes of this report, but an accurate theoretical description of repeated inelastic loading and unloading of Mohr-Coulomb materials must be more rigorous and will require further theoretical work.

CHAPTER 3

EVALUATION OF THE THEORY

3.1 COMPARISON OF CALCULATIONS WITH EXPERIMENTAL EVIDENCE

Calculations were made for small-scale tests conducted by the Stanford Research Institute (SRI) (Reference 4) to evaluate the theory of this report. In these experiments explosives were used in a specially designed device to produce axially symmetric loads. Displacements as a function of time were measured using the "light ring" technique which consists of photographing the motion of the inner pipe wall by means of a bright ring of light transmitted through a transparent flexible plastic tube glued to the pipe wall. The targets considered for calculation were 3-inch-OD tubes of "super lean grout" (SLG) lined with a 10-mil-thick pipe of Type 347 stainless steel. The material properties used in the calculations are given in Table 3.1.

Figure 3.1 shows data from two shots with 80 grams of explosive. The estimated free-field pressure pulse obtained from calibration tests is also shown in the figure. Calculated curves are for Poisson's ratio, $\nu = 0.25$, 0.38 , and 0.5 , where 0.38 was the value of ν calculated from ultrasonic velocity measurements in SLG given in Reference 5. There is good agreement between the theory and experiment. Figure 3.2 presents measurements from three shots with estimated free-field pressure pulses as shown. Here the calculated values are close to the experimental points, but the agreement is not as good as in Figure 3.1.

An additional check of the theory can be obtained by noting that the internal resistance $R = KU - Y$ is the static stress-strain curve. Thus data from static or quasi-static tests can be used to evaluate this important part of the dynamic equation of motion (Equation 2.16). Figure 3.3 shows static calculations compared with measurements obtained by SRI.¹ In this test a hydrostatic load was applied to a sample of

¹ Letter of 10 Jun 1975 from T. C. Kennedy, Stanford Research Institute, Menlo Park, Calif., to J. Drake, Weapons Effects Laboratory, U. S. Army Engineer Waterways Experiment Station, CE, Vicksburg, Miss.

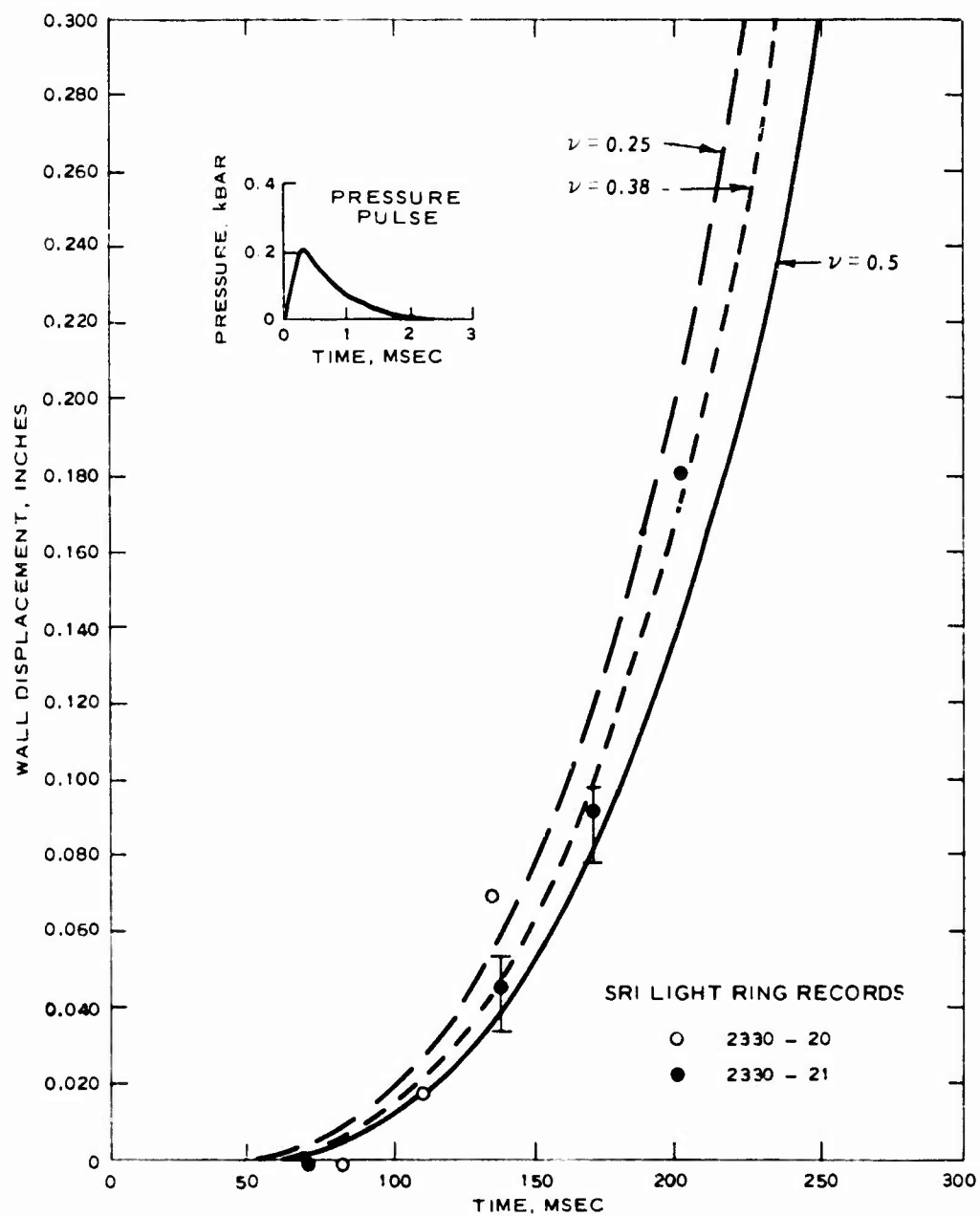


Figure 3.1 Calculated displacement-time curves compared with measurements with 80-gram charges (from Reference 4).

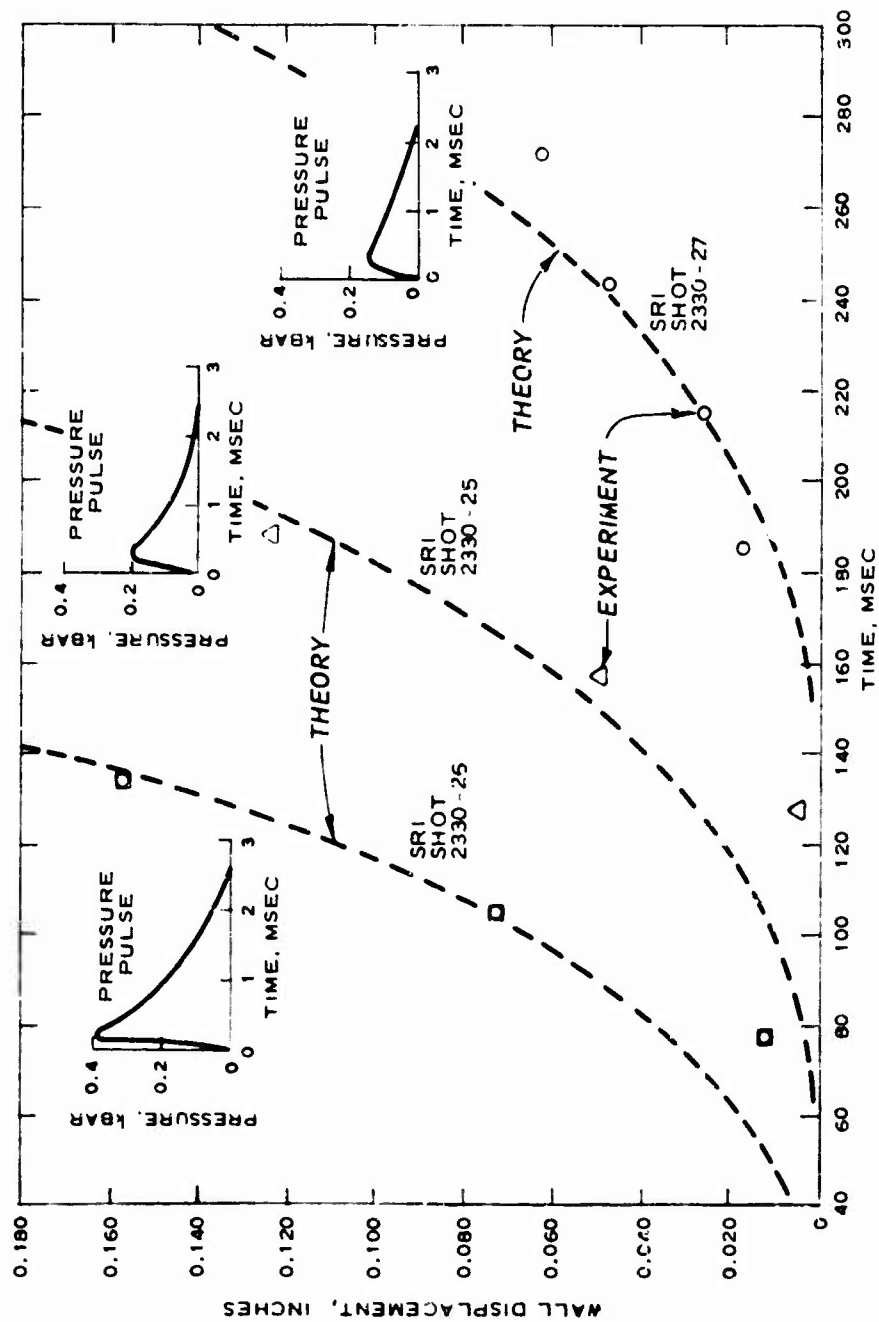


Figure 3.2 Theoretical and experimental wall displacements versus time for three pressure pulses (from Reference 4).

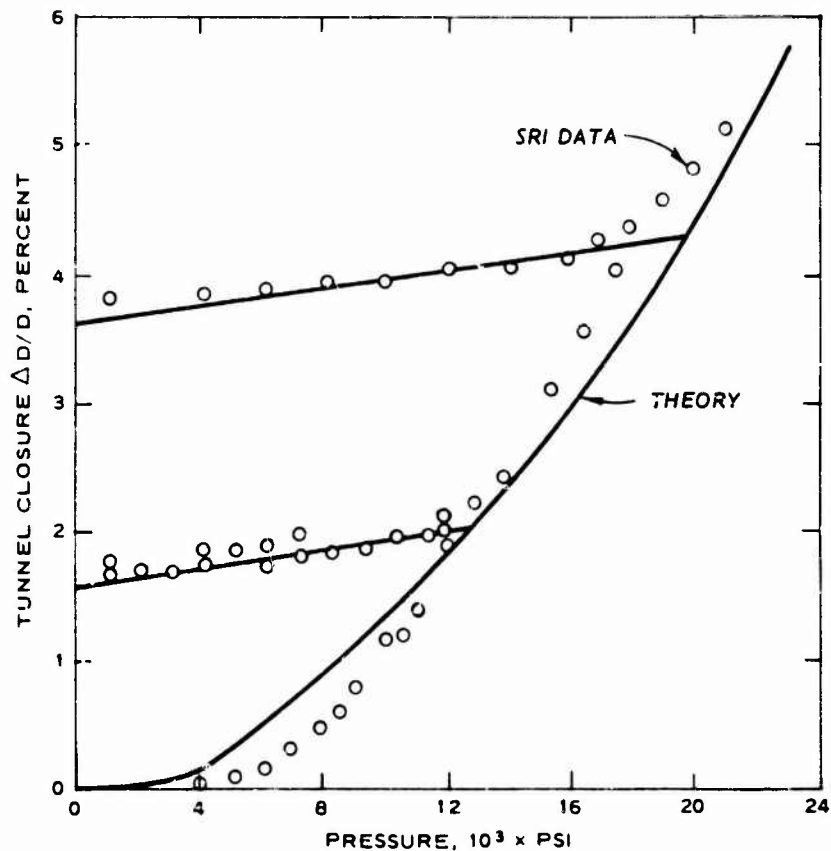


Figure 3.3 Computed and measured static tunnel closure versus pressure.

WES 6B rock simulant containing a 0.625-inch-ID tunnel lined with a 0.025-inch-thick mild steel tube. The material properties used in the calculation are given in Table 3.1. The displacement or tunnel closure is expressed as a percentage of the inside diameter D of the tunnel. The calculated unload curves assumed elastic behavior. Again, there is good agreement between theory and experiment.

3.2 CONCLUSIONS

An analysis has been presented which extends the static methods outlined by Newmark (Reference 1) to accommodate dynamic loads. Comparisons of calculations with experimental data have demonstrated that the analysis will predict satisfactorily the time-displacement curve in uniform radial load for materials which can be modeled as elastic-plastic

media having a Mohr-Coulomb or von Mises yield criterion. The analysis given in this report is in a form which allows quick, inexpensive preliminary design calculations for deep underground structures.

Users of the theory must be warned, however, that the analysis will not predict accurately displacements for biaxial loads where the vertical and horizontal normal stress components are significantly different or where a large amount of ovaling of the tunnel liner may be expected. In this case the theory will provide a conservative lower bound estimate of the deformation. At present, a design method for biaxial loading is not available in a relatively simple form comparable with the analysis procedure outlined in this report. Work in this area is needed.

The present analysis is limited to monotonically increasing displacements. In the case of small plastic strains, unload and a subsequent reload may take place elastically. This process can be treated simply within the present analysis.

TABLE 3.1 MATERIAL PROPERTIES USED IN THE CALCULATIONS

Material	Shear Modulus G 10^6 psi	Poisson's Ratio ν	Cohesion c 10^3 psi	Angle of Internal Friction ϕ degrees	Density ρ 10^{-4} psi in./sec ²
Super lean grout	0.058	0.38	0.016	0.7	1.65
347 stainless steel	11.2	0.3	20	0	7.5
WES 6B rock simulant	0.48	0.25	1.7	30	--
Mild steel	12	0.3	20	0	--

REFERENCES

1. N. M. Newmark; "Design of Rock Silo and Rock Cavity Linings"; Technical Report TR 70-114, August 1969; Space and Missiles Systems Organization, Air Force Systems Command, Norton Air Force Base, Calif.
2. A. J. Hendron, Jr., and A. K. Aiyer; "Stresses and Strains Around a Cylindrical Tunnel in an Elasto-Plastic Material with Dilatancy"; Technical Report 10, September 1972; U. S. Army Engineer District, Omaha, CE, Omaha, Nebr.
3. W. Prager and P. G. Hodge; "Theory of Perfectly Plastic Solids"; 1951; John Wiley and Sons, New York, N. Y.
4. R. W. Gates, C. F. Petersen, and A. L. Florence; "Laboratory Method for Studying Stemming of Line-of-Sight Tunnels in Underground Nuclear Tests"; Report PYU-2330 (DNA-3592F), December 1973; Stanford Research Institute, Menlo Park, Calif.
5. S. W. Butters and others; "Material Properties of Grouts and of Tuffs from Selected Drill Holes"; Technical Report TR-73-69 (DNA-3383F), July 1974; Terra Tek, Salt Lake City, Utah.

APPENDIX A: NOTATION

C_i	An integration constant in the radial stress solution
G_i	Shear modulus
i	A subscript or superscript referring to a component material in the cross section
K	Effective elastic stiffness
m	Number of materials in the cross section
M	Effective mass
n_i	$N_i - 1$
N_i	$(1 + \sin \phi_i)/1 - \sin \phi_i$
$p(t)$	Exterior pressure-time history (compressive)
$p_o(t)$	Interior pressure (compressive)
$P_o(t)$	Effective interior pressure in equation of motion
p_1, p_2	Inside and outside applied load, respectively
q_i	Cohesion
r	Radial coordinate
r_i	Interior boundary of the i^{th} material layer
r_1, r_2	Inside and outside radii, respectively
R	Internal resistance
S^i	Mean normal stress
t	Time
u_c/u_i	Ratio of the compressible to the incompressible radial displacements
u_r^i, u_θ^i	Radial and tangential displacement components, respectively
U	Displacement potential
Y	Effective rigid plastic collapse pressure of the m materials
$\epsilon_r^i, \epsilon_\theta^i$	Radial and tangential strain components, respectively
ν	Poisson's ratio
ρ_i	Density
$\sigma_r^i, \sigma_\theta^i, \sigma_z^i$	Radial, tangential, and axial stress components, respectively
ϕ_i	Angle of internal friction

DISTRIBUTION LIST FOR MISCELLANEOUS PAPER N-76-9

<u>Address</u>	<u>No. of Copies</u>
<u>OCE</u>	
Headquarters, Department of the Army Washington, D. C. 20314	
ATTN: DAEN-ASI-L	2
DAEN-MCE-D	1
DAEN-MCE	1
DAEN-MCE-D/Mr. D. S. Reynolds	1
DAEN-RDL	1
DAEN-CWE	1
<u>District and Division Offices</u>	
Division Engineer	1
U. S. Army Engineer Division, Huntsville P. O. Box 1600, West Station, Huntsville, Ala. 35807	
U. S. Army Engineer Division, Huntsville P. O. Box 1600, West Station, Huntsville, Ala. 35807	
ATTN: HNDED-CS/Mr. Michael M. Dembo	2
HNDED-SR	2
Division Engineer	1
U. S. Army Engineer Division, Lower Mississippi Valley P. O. Box 80, Vicksburg, Miss. 39180	
Division Engineer	
U. S. Army Engineer Division, Missouri River P. O. Box 103, Downtown Station, Omaha, Nebr. 68101	
ATTN: Library	3
Division Engineer	1
U. S. Army Engineer Division, North Atlantic 90 Church Street, New York, N. Y. 10007	
Division Engineer	
U. S. Army Engineer Division, North Atlantic 90 Church Street, New York, N. Y. 10007	
ATTN: NADEN/Chief, Engineering Division	1
Division Engineer	1
U. S. Army Engineer Division, North Central 536 South Clark Street, Chicago, Ill. 60605	

Address	No. of Copies
<u>District and Division Offices (Continued)</u>	
Division Engineer U. S. Army Engineer Division, North Pacific 210 Custom House, Portland, Oreg. 97209	1
Division Engineer U. S. Army Engineer Division, Ohio River P. O. Box 1159, Cincinnati, Ohio 45201	1
Division Engineer U. S. Army Engineer Division, Ohio River P. O. Box 1159, Cincinnati, Ohio 45201 ATTN: Division Laboratory, ORDED-FL	1
Division Engineer U. S. Army Engineer Division, South Atlantic 510 Title Building, 30 Pryor Street, SW. Atlanta, Ga. 30303	1
Division Engineer U. S. Army Engineer Division, South Pacific 630 Sansome Street, Room 1216, San Francisco, Calif. 94111	1
Division Engineer U. S. Army Engineer Division, Southwestern Main Tower Building, 1200 Main Street, Dallas, Tex. 75202	1
<u>Army</u>	
Defense Documentation Center Cameron Station, Alexandria, Va. 22314 ATTN: TC/Mr. Myer B. Kahn	12
Director U. S. Army Coastal Engineering Research Center Kingman Building, Fort Belvoir, Va. 22060 ATTN: Librarian	1
Commander/Director U. S. Army Cold Regions Research and Engineering Laboratory P. O. Box 282, Hanover, New Hampshire 03755 ATTN: Library	1
Director U. S. Army Construction Engineering Research Laboratory P. O. Box 4005, Champaign, Ill. 61820 ATTN: Library	1

<u>Address</u>	<u>No. of Copies</u>
<u>Army (Continued)</u>	
Commander U. S. Army Mobility Equipment R&D Center Fort Belvoir, Va. 22060 ATTN: Technical Documents Center, Building 315	1
Commandant U. S. Army Engineer School Fort Belvoir, Va. 22060 ATTN: Department of Engineering Secretary	1 1
Commander U. S. Army Mobility Equipment R&D Center Fort Belvoir, Va. 22060 ATTN: Technical Library	1
Commander U. S. Army Missile Command Redstone Scientific Information Center Redstone Arsenal, Ala. 35809 ATTN: Chief, Documents	1
Commander U. S. Army Forces Command Fort McPherson, Ga. 30330 ATTN: AFEN-FEB AFEN (Mil Engr Div)	1 1
138th Engineer Group (Construction) Department of the Army Fort Riley, Kans. 66442 ATTN: ALBFEN-O	1 1
Commandant U. S. Army Command and General Staff College Fort Leavenworth, Kans. 66027 ATTN: ATSW-RI-L	1
Commander Harry Diamond Laboratories 2800 Powder Mill Road Adelphi, Md. 20783 ATTN: AMXDO-NP, Mr. Louis Belliveau/Mr. J. H. Gwaltney	1

Address	No. of Copies
<u>Army (Continued)</u>	
Director U. S. Army Ballistic Research Laboratories Aberdeen Proving Ground, Md. 21005 ATTN: AMXBR-X/Mr. J. J. Meszaros	1
Commander U. S. Army Electronics Command Fort Monmouth, N. J. 07703 ATTN: AMSEL-GG-TD	1
Commanding Officer Picatinny Arsenal Dover, N. J. 07801 ATTN: ORDBR-TK	1
Chief, Plastics Technical Evaluation Center	1
SARPA-TS-S/No. 59	1
P. Angelloti	1
SMUPA-ND-S/Mr. E. Zimpo	1
Superintendent U. S. Military Academy West Point, N. Y. 10996 ATTN: Library	2
U. S. Military Academy Department of Engineering West Point, N. Y. 10996 ATTN: MADN-F	1
President U. S. Army Air Defense Board Fort Bliss, Tex. 79916	1
Commandant U. S. Army Air Defense School Fort Bliss, Tex. 79916	1
Commander U. S. Army Nuclear Agency Fort Bliss, Tex. 79916 ATTN: ATCANA-W	1
Director Eustis Directorate, U. S. Army Air Mobility Research and Development Laboratory Fort Eustis, Va. 23604 ATTN: SAVDL-EU-MOS (Room 209)	1

Address	No. of Copies
<u>Army (Continued)</u>	
Commander U. S. Army Training and Doctrine Command Fort Monroe, Va. 23351 ATTN: ATEN-ME	1
Commandant Armed Forces Staff College Norfolk, Va. 23511 ATTN: Library	1
Commander U. S. Army Materiel Development and Readiness Command (DARCOM) 5001 Eisenhower Avenue Alexandria, Va. 22333 ATTN: DACRD-WN	2
Office, Chief of Research, Development, and Acquisition (DAMA-CSS-D) Department of the Army Washington, D. C. 20310 ATTN: Mr. Paul F. Carlton	1
Technical Library	3
<u>Navy</u>	
Commanding Officer and Director U. S. Naval Electronics Laboratory San Diego, Calif. 92152	1
Commander Naval Weapons Center China Lake, Calif. 93555	1
Superintendent U. S. Naval Postgraduate School Monterey, Calif. 93940 ATTN: Library, Code 2124	1
Commander Naval Weapons Center China Lake, Calif. 93555 ATTN: Peggy Davis, Code 4503	1

Address	No. of Copies
<u>Navy (Continued)</u>	
Officer in Charge Civil Engineering Laboratory Naval Construction Battalion Center Port Hueneme, Calif. 93043 ATTN: Code L31	1
Commanding Officer Nuclear Weapons Training Group, Pacific U. S. Naval Station, North Island San Diego, Calif. 92135	1
Commanding Officer and Director Naval Ship Research and Development Center Bethesda, Md. 20084 ATTN: Code 5641	1
Commander Naval Surface Weapons Center, White Oak Silver Springs, Md. 20910 ATTN: 243 240 241	1 1 1
Underwater Explosions Research Division Naval Ship Research and Development Center Norfolk Naval Shipyard Portsmouth, Va. 23709	1
Commander Naval Surface Weapons Center, Dahlgren Laboratory Dahlgren, Va. 22448 ATTN: MAL	1
Commander Naval Facilities Engineering Command Department of the Navy Hoffman Building, 200 Stovall Street Alexandria, Va. 22332 ATTN: NFAC-04B NFAC-03	1 1
Chief of Naval Research Navy Department Arlington, Va. 22217 ATTN: Code 464	1

<u>Address</u>	<u>No. of Copies</u>
<u>Navy (Continued)</u>	
Commanding Officer Nuclear Weapons Training Center Atlantic Naval Base Norfolk, Va. 23511 ATTN: Nuclear Warfare Department	1
Commander-in-Chief U. S. Atlantic Fleet U. S. Naval Base Norfolk, Va. 23511	1
Commander U. S. Naval Oceanographic Office Washington, D. C. 20373 ATTN: Library, Code 1600	1
Chief of Naval Operations Navy Department Washington, D. C. 20350 ATTN: OP-75	1
Director Naval Research Laboratory Washington, D. C. 20375 ATTN: Code 2627	1
Special Projects Navy Department Washington, D. C. 20360 ATTN: SP-272	1
Commander Naval Ordnance Systems Command Navy Department Washington, D. C. 20360	1
Commander Naval Ship Engineering Center Navy Department Washington, D. C. 20360 ATTN: Code 6105	1
Commanding General Marine Corps Dev and Education Command Quantico, Va. 22134 ATTN: Director, Development Center	2

Address	No. of Copies
<u>Navy (Continued)</u>	
Commandant of the Marine Corps Washington, D. C 20380 ATTN: Code RD	2
<u>Air Force</u>	
Commander Space and Missile Systems Organization Norton Air Force Base, Calif. 92409 ATTN: MNNH/CPT J. V. Kaiser, Jr. DEB	2 1
Director, USAF Project Rand Via: U. S. Air Force Liaison Officer The Rand Corporation 1700 Main Street Santa Monica, Calif. 90406 ATTN: Library	1
Air Force Technical Applications Center/Tr Patrick Air Force Base, Fla. 32925	1
Commander JSTPS/JLPW (ATTN: LCDR M. Barrata) Offutt Air Force Base, Nebr. 68113	1
Commander Strategic Air Command Offutt Air Force Base, Nebr. 68113 ATTN: OAWS	1
Commander Air Force Weapons Laboratory, AFSC Kirtland Air Force Base, N. Mex. 87117 ATTN: DEV-G/Mr. R. W. Henny DEV-G/MAJ J. T. Neal DEV-S/MAJ James M. Warren DEV/CPT G. W. Ullrich SUL, Technical Library DEV-S/Dr. M. A. Plamondon Steve Melzer DEV-F/Mr. J. L. Bratton	1 1 1 1 1 1 1 1
Air Force Institute of Technology AFIT Bldg 640 Area B Wright-Patterson Air Force Base, Ohio 45433 ATTN: Technical Library	1

Address	No. of Copies
<u>Air Force (Continued)</u>	
Commander Air Force Logistics Command Wright-Patterson Air Force Base, Ohio 45433	2
Langley Research Center NASA, Langley Field Hampton, Va. 23665 ATTN: Mr. Philip Donely	1
Headquarters, TAC/INTT Langley Air Force Base, Va. 23665	1
Director of Civil Engineering Headquarters, Air Force Systems Command Andrews Air Force Base Washington, D. C. 20331 ATTN: DEE	1
Director of Civil Engineering Headquarters, USAF Washington, D. C. 20330 ATTN: AF/PREE	1
<u>APO and FPO</u>	
Commander-in-Chief, Pacific FPO San Francisco, Calif. 94129	1
U. S. Documents Officer Office of the United States National Military Representative-Chape APO New York, N. Y. 09055	1
<u>Domestic Exchanges</u>	
Northern Arizona University Box 15600 Flagstaff, Ariz. 86001 ATTN: Prof. Sandor Popovics	1
<u>Other Government Agencies</u>	
Director Lawrence Livermore Laboratory P. O. Box 808, Livermore, Calif. 94550 ATTN: K-Division	1

Address	No. of Copies
<u>Other Government Agencies (Continued)</u>	
U. S. Department of the Interior U. S. Geological Survey 345 Middlefield Road Menlo Park, Calif. 94025 ATTN: Mr. Harold W. Olsen	1
Director Lawrence Livermore Laboratory P. O. Box 808 Livermore Calif. 94550	1
Director Lawrence Livermore Laboratory Technical Information Division P. O. Box 808 Livermore, Calif. 94550 ATTN: Technical Library	1
Ms. Barbara Germain	1
Manager Albuquerque Operations Office U. S. Energy Research and Development Administration P. O. Box 5400 Albuquerque, N. Mex. 87115	1
Commander, Field Command Defense Nuclear Agency Kirtland Air Force Base, N. Mex. 87115 ATTN: FCTD, Director	1
FCPR	1
Sandia Laboratories P. O. Box 5800 Albuquerque, N. Mex. 87115 ATTN: Technical Library	1
Commander Field Command, Defense Nuclear Agency Kirtland Air Force Base, N. Mex. 87115 ATTN: FCTD-T	1
Sandia Laboratories P. O. Box 5800 Albuquerque, N. Mex. 87115 ATTN: Doc Control for Mr. L. J. Vortman	1

<u>Address</u>	<u>No. of Copies</u>
<u>Other Government Agencies (Continued)</u>	
Los Alamos Scientific Laboratory P. O. Box 1663, Los Alamos, N. Mex. 87544 ATTN: Document Control for Reports Library	1
Sandia Laboratories P. O. Box 5800, Albuquerque, N. Mex. 87115 ATTN: John Kaiser	1
Director Defense Advanced Research Projects Agency Architect Building, 1400 Wilson Blvd. Arlington, Va. 22209 ATTN: NTDO	1
Administrator National Aeronautics and Space Adm. Washington, D. C. 20546 ATTN: Marine Transportation Officer (Code BXC)	1
National Military Command Systems Support Center Pentagon BE 685 Washington, D. C. 20301 ATTN: Technical Library	1
Director of Defense Research and Engineering Washington, D. C. 20301 ATTN: Technical Library, Room 3C-128 Mr. Frank J. Thomas	1 1
Federal Highway Administration Department of Transportation Chief, Structural and Applied Mechanics Division Washington, D. C. 20590 ATTN: Mr. F. J. Tamanini	1
Director Defense Intelligence Agency Department of Defense Washington, D. C. 20301 ATTN: DI-7D	1
Director Defense Civil Preparedness Agency Washington, D. C. 20301 ATTN: Mr. George Sison (RE-HV)	1

<u>Address</u>	<u>No. of Copies</u>
<u>Other Government Agencies (Continued)</u>	
Director Defense Nuclear Agency Washington, D. C. 20305 ATTN: SPSS	5
Director Weapons Systems Evaluation Group Washington, D. C. 20305	1
U. S. Energy Research and Development Administration Technical Information Service Washington, D. C. 20545 ATTN: Chief, Classified Technical Library	1
<u>Colleges and Universities</u>	
University of Arizona College of Engineering Tucson, Ariz. 85721 ATTN: Dr. George Howard	1
University of Colorado School of Architecture Boulder, Colo. 80304 ATTN: Prof. G. K. Vetter	1
University of Detroit Department of Civil Engineering 4001 West McNichols Road Detroit, Mich. 48221 ATTN: Prof. Warren J. Baker	1
George Washington University Nuclear Defense Design Center School of Engineering and Applied Science Washington, D. C. 20052 ATTN: Prof Raymond R. Fox	1
George Washington University Nuclear Defense Design Center School of Engineering and Applied Science Washington. D. C. 20006	1

Address	No. of Copies
<u>Colleges And Universities (Continued)</u>	
University of Illinois Civil Engineering Building, Urbana, Ill. 61801 ATTN: Metz Reference Room, B106	1
Prof. W. J. Hall	1
Prof. A. J. Hendron, Jr.	1
Dr. Nathan M. Newmark, 1211	1
Iowa State University of Science and Technology 231 Sweeney Hall, Ames, Iowa 50010 ATTN: Prof. Glenn Murphy	1
Lehigh University Department of Civil Engineering Bethlehem, Pa. 18015 ATTN: Dr. D. A. Van Horn	1
University of Massachusetts Department of Civil Engineering Amherst, Mass. 01002 ATTN: Dr. M. F. White	1
Massachusetts Institute of Technology 77 Massachusetts Avenue, Room 1-382, Cambridge, Mass. 02139 ATTN: Dr. R. V. Whitman	1
University of Michigan Department of Civil Engineering 304 West Engineering, Ann Arbor, Mich. 48104 ATTN: Prof. F. E. Richart, Jr.	1
University of Missouri - Rolla Rock Mechanics and Explosives Research Center Buehler Building, Rolla, Mo. 65401 ATTN: Dr. George B. Clark, Director	1
University of New Mexico Eric H. Wang Civil Engineering Research Facility P. O. Box 188, University Station, Albuquerque, N. Mex. 87106	2
Pennsylvania State University 101 Eng. A University Park, Pa. 16802 ATTN: Prof. Richard Kummer	1

Address	No. of Copies
<u>Colleges and Universities (Continued)</u>	
Pennsylvania State University Department of Architectural Engineering University Park, Pa. 16802 Prof. G. Albright, Head	1
Purdue University School of Civil Engineering Civil Engineering Building, Lafayette, Ind. 47907 Prof. M. B. Scott	1
Rensselaer Polytechnic Institute Mason House, Troy, N. Y. 12180 ATTN: Dr. Clayton Oliver Dohrenwend, Security Officer	1
Rice University Department of Civil Engineering P. O. Box 1892, Houston, Tex. 77001 ATTN: Prof. A. S. Veletsos	1
San Jose State College Department of Civil Engineering San Jose, Calif. 95114 ATTN: Dr. Robert G. Spicher	1
University of Texas at Austin Balcones Research Center Route 4, Box 189, Austin Tex. 78757 ATTN: Dr. J. Neils Thompson	1
Utah State University Department of Mechanical Engineering Logan, Utah 84321 ATTN: Prof. R. K. Watkins	1
University of Washington Department of Civil Engineering FX-10, Seattle, Wash. 98195 ATTN: Chairman	1
Worcester Polytechnic Institute Department of Civil Engineering Worcester, Mass. 01609 ATTN: Dr. Carl Koontz	1

Address	No. of Copies
<u>Corporations</u>	
Aerospace Corporation P. O. Box 92957, Los Angeles, Calif. 90009 ATTN: Dr. Prem N. Mathur	1
Agbabian Associates Engineering Consultants 250 North Nash Street, El Segundo, Calif. 90245	2
Applied Theory Incorporated 1010 Westwood Boulevard, Los Angeles, Calif. 90024 ATTN: Dr. John G. Trulio	1
AVCO Corporation Research and Advanced Development Division 201 Lowell Street, Wilmington, Mass. 01887 ATTN: Mr. R. E. Cooper	1
Bell Telephone Laboratories Outside Structures Department Whippany, N. J. 07981 ATTN: Mr. John Foss	1
The Boeing Company P. O. Box 3707, Seattle Wash. 98124 ATTN: Technical Library	1
Battelle Columbus Laboratories 505 King Avenue, Columbus, Ohio 43201 ATTN: Dr. P. N. Lamori	1
Energy Incorporated P. O. Box 736, Idaho Falls, Idaho 83401	1
General Research Corporation Document Control Supervisor Westgate Research Park, McLean, Va. 22101	1
General Electric Company, Tempo 816 State Street, Santa Barbara, Calif. 93102 ATTN: Mr. Warren Chan (DASIAC)	1
General Electric Company Space and RESD Division P. O. Box 8555, Philadelphia, Pa. 19101 ATTN: Larry Chasen, Manager-Libr.	1

Address	No. of Copies
<u>Corporations (Continued)</u>	
General Research Corporation P. O. Box 3587 Santa Barbara, Calif. 93105 ATTN: Mr. Benjamine Alexander	1
Dr. John S. Rinehart Hyperdynamics P. O. Box 392, Santa Fe, N. Mex. 87501	1
IIT Research Institute 10 West 35th Street, Chicago, Ill. 60616 ATTN: Dr. T. Schiffman	1
Martin Marietta Aerospace, Orlando Division P. O. Box 5837, Orlando, Fla. 32805 ATTN: Gerbert E. McQuaig (MP 18)	1
Physics International Company 2700 Merced Street, San Leandro, Calif. 94577 ATTN: DOC Control for Dr. Charles Godfrey DOC Control for Mr. Fred M. Sauer	1 1
R&D Associates P. O. Box 9695, Marina Del Rey, Calif. 90291 ATTN: Dr. Harold L. Brode Dr. H. F. Cooper, Jr. Dr. Bruce Hartenbaum Mr. J. G. Lewis	1 1 1 1
The Rand Corporation 1700 Main Street Santa Monica, Calif. 90406	1
Southwest Research Institute 8500 Culebra Road, San Antonio, Tex. 78228 ATTN: Dr. Robert C. Dehart	1
Systems, Science and Software P. O. Box 1620, La Jolla, Calif. 92307 ATTN: Dr. Donald R. Grine Dr. T. R. Blake	1 1
Electromechanical Systems of New Mexico, Inc. P. O. Box 11730, Albuquerque, N. Mex. 87112 ATTN: R. A. Shunk	1

Address	No. of Copies
<u>Corporations (Continued)</u>	
Stanford Research Institute 333 Ravenswood Avenue Menlo Park, Calif. 94025 ATTN: Dr. G. Abrahamson	1
Terra Tek, Inc. University Research Park 420 Wakara Way Salt Lake City, Utah 84108 ATTN: Mr. S. J. Green	1
Weidlinger Associates, Consulting Engineers 110 East 59th Street New York, N. Y. 10022 ATTN: Dr. Melvin L. Baron	1
<u>Foreign</u>	
Chief Superintendent Defense Research Establishment Suffield Ralston, Alberta, Canada	1
Ministry of Defense (Engineer Equipment) MVEE (Christchurch) Hampshire, England ATTN: Dr. Philip S. Bulson	1
Dr. K.-J. Melzer c/o Battelle-Institut e. V. P. O. Box 900160, 6 Frankfurt/Main 90, Germany-West	1

In accordance with ER 70-2-3, paragraph 6c(1)(b), dated 15 February 1973, a facsimile catalog card in Library of Congress format is reproduced below.

Drake, James L

A method for designing deep underground structures subjected to dynamic loads, by James L. Drake and James R. Britt. Vicksburg, U. S. Army Engineer Waterways Experiment Station, 1976.

45 p. illus. 27 cm. (U. S. Waterways Experiment Station. Technical report N-76-9)

Prepared for Defense Nuclear Agency, Washington, D. C., and Office, Chief of Engineers, U. S. Army, Washington, D. C., under DNA Subtask J34CAXSX311, "Underground Structures Studies," and OCE Project 4A762719AT40/A1/017, "Stability of Deep Underground Structures in Rock."

References: p. 27.

1. Dynamic loads. 2. Underground structures.

I. Britt, James R., joint author. II. Defense Nuclear Agency. III. U. S. Army. Corps of Engineers. (Series: U. S. Waterways Experiment Station, Vicksburg, Miss. Technical report N-76-9)
TA7.W34 no N-76-9